Accepted Manuscript

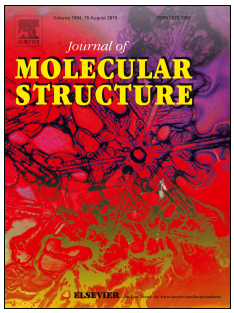

Modulation of dual fluorescence modes and emissions of 2-(1,4-dioxo-1,4-dihydro-naphthalen-2-yl-amino)benzoic acid

Munendra Pal Singh, Jubaraj B. Baruah

PII: S0022-2860(17)31058-X

DOI: 10.1016/j.molstruc.2017.08.004

Reference: MOLSTR 24141

To appear in: *Journal of Molecular Structure*

Received Date: 14 July 2017

Revised Date: 1 August 2017

Accepted Date: 2 August 2017

Please cite this article as: M.P. Singh, J.B. Baruah, Modulation of dual fluorescence modes and emissions of 2-(1,4-dioxo-1,4-dihydro-naphthalen-2-yl-amino)benzoic acid, *Journal of Molecular Structure* (2017), doi: 10.1016/j.molstruc.2017.08.004.

Graphical abstract

Modulation of dual fluorescence modes and emissions of 2-(1,4-dioxo-1,4-dihydro-napthalen-2-yl-amino)benzoic acid

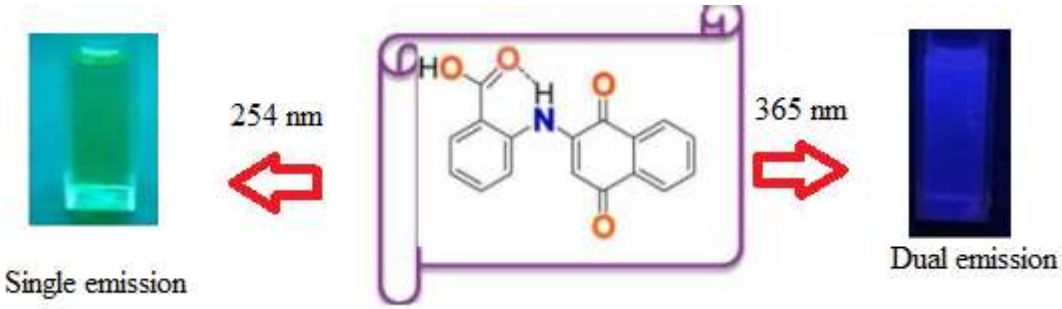

Excitation of solutions of 2-(1,4-dioxo-1,4-dihydronapthalen-2-yl-amino)benzoic acid in UV-region shows single emission whereas excitation in visible region shows dual emission

Munendra Pal Singh and Jubaraj B. Baruah

Graphical TOC

Modulation of dual fluorescence modes and emissions of 2-(1,4-dioxo-1,4-dihydro-naphthalen-2-yl-amino)benzoic acid

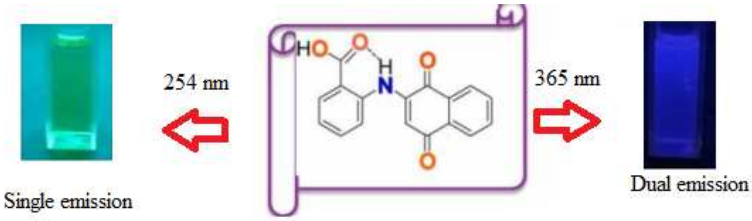

Excitation of solutions of 2-(1,4-dioxo-1,4-dihydronaphthalen-2-yl-amino)benzoic acid in UV-region shows single emission whereas excitation in visible region shows dual emission

Munendra Pal Singh and Jubaraj B. Baruah

Modulation of dual fluorescence modes and emissions of 2-(1,4-dioxo-1,4-dihydro-naphthalen-2-yl-amino)benzoic acid

Munendra Pal Singh and Jubaraj B. Baruah*

Department of Chemistry, Indian Institute of Technology Guwahati, Guwahati 781 039 Assam, India; email: juba@iitg.ernet.in, phone +91-361-2311; Fax +91-361-2690762

Abstract:

Intra-molecularly hydrogen bonded compound 2-(1,4-dioxo-1,4-dihydronaphthalen-2-yl-amino)benzoic acid (ANQ) shows emission at single wavelength upon excitation in UV-region whereas it shows dual fluorescence emissions on excitation in visible region. Such emissions depend on solvent, concentration and pH. Solvent dependent structural changes of ANQ are reflected in solution studies carried out by ^{1}HNMR, UV-visible and fluorescence spectroscopy. DLS study has showed that in addition to monomers, self-assemblies with 415 nm average sized particles are formed in DMF solution. HOMO-LUMO of three tautomeric forms of the compound was calculated by DFT using CAMB3LYP/6-31+G(d,p) as basis set shows that naphthoquinone form has about 86.30 KJ/mol higher stability over an imino-quinone form. From various studies relating concentration dependence, pH, life-time, study on dual-emissions caused by visible excitation has established the observed emissions to originate from aggregation contributing as charge-transfer and deprotonated species. Whereas

the single emission caused by UV-excitation occurs through excited state intra-molecular proton transfer.

Keywords: Dual-modes; Dual-emissions; Amino-naphthoquinone; Intra-molecular hydrogen bond; Fluorescence modulation.

Introduction

Fluorescence emissions of small-molecules are extensively used as biological probes [1]. Advantages from small molecules that show environment sensitive fluorescence are taken to use them as biological probes to understand micro-environmental changes due to protein conformational changes [2-3]. There are also situations in which a molecule may not induce enough environmental changes to cause a noticeable difference to fluorescence probe [4]; hence fluorescence properties associated with a potential probe requires thorough attention. Interactions of small molecules [5-9] with proteins and DNA are routinely explored. In our recent study we found wide variations in binding abilities of 2-(1,4-dioxo-1,4-dihydronaphthalen-2-yl-amino)benzoic acid causing fluorescence emission changes to human serum albumin in comparison to the positional isomer 4-(1,4-dioxo-1,4-dihydronaphthalen-2-yl-amino)benzoic acid [10]. Among small fluorescent molecules quinone derivatives are ubiquitous in electron transfer [11-17], ion-recognition [18-25] and in electrochemistry [26-29]. Many quinone derivatives are used as fluorescence probes [30-38] and some of them show non-linear optical property [39]. Fluorescent quinone derivatives are useful in ion detection and to modulate fluorescence by ions [40-41]. Quinone linked photo-active peptides have interesting photophysical properties [42]. Certain quinones show fluorescence emission at two different wavelengths when excited by single wavelength [43]. It is interesting to note

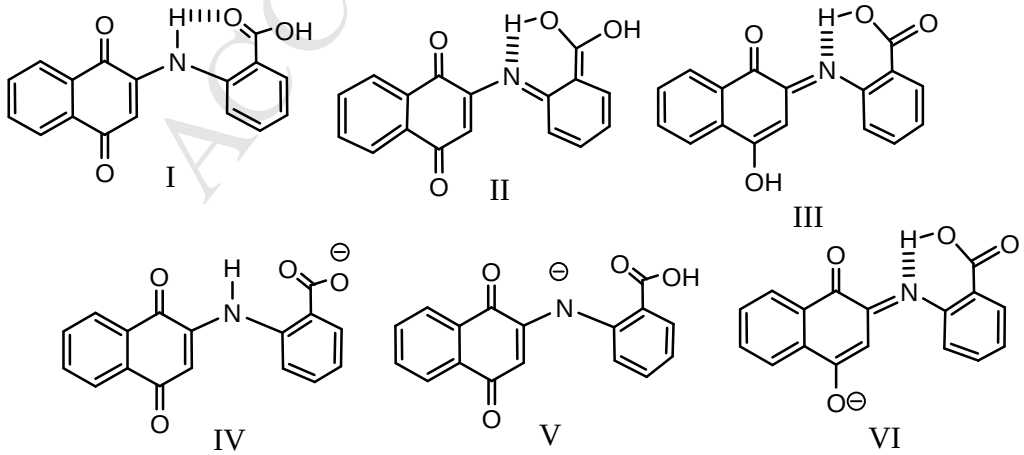

Fig. 1: Some probable forms of ANQ in neutral and basic conditions.

that certain compounds possessing keto-imine forms show dual fluorescence [44-46]. Keto-enol tautomers of hydroxyquinones [47] and keto-imine forms of aminoquinones [48] are well known but less explored for fluorescence study. Recently dual-emissions were observed by us while exciting at UV- or visible region in inter-molecular hydrogen-bonded 4-aminobenzoic acid tethered 1,4-naphthoquinone [49]. It may be noted that 2-(1,4-dioxo-1,4-dihydronaphthalen-2-yl-amino)benzoic acid (ANQ) showed relatively lower binding towards bovine serum albumin protein in comparison to a series of analogous naphthoquinone derivatives. This is an interesting point to note, as weakly bound fluorescence probe will be easy to manipulate in biological conditions. It is worth noting that diethylamino-2-hydroxybenzaldehyde shows dual emission through suppression of intramolecular charge-transfer by excited state proton transfer process [50]. Thus, ANQ is chosen to explore interesting emission features from different intramolecular hydrogen bonded structural forms shown in Fig. 1 (I-III). Depending on pH anionic species of ANQ such as IV-VI shown in Fig. 1 are also possible, which may in turn contribute to emission process. Different tautomeric forms of ANQ in solution should prefer single emission path or combined emission paths under different conditions. Accordingly understanding of fluorescence properties of ANQ under different conditions is of interest. With this background we explored fluorescence emission properties of ANQ to understand independent or collective contribution of forms I-V to fluorescence emissions under different conditions.

Experimental:

Infrared spectra were obtained using Perkin-Elmer FT-IR spectrophotometer (KBr, 4000-400 cm^{-1}). UV-Vis-spectra were recorded using Perkin-Elmer Lambda 750 UV-Visible spectrophotometer. Fluorescence emissions were measured in a Perkin-Elmer LS-55 spectrofluorimeter by taking appropriate amount of solutions of the compound (3mL in each case) in different conditions. NMR spectra were recorded in Varian-AS400 (oxford) 400MHz and Bruker 600MHz NMR spectrometer. ESI-mass spectra were recorded on a liquid chromatography mass spectrometer using Water Q-TOF premier mass spectrometer attached to aquity HPLC. Life-time decay profiles were measured on an Eddinburg Instrument, Model: FSP920. Dynamic light scattering (DLS) experiments were performed with a Malvern Zetasizer Nano ZS instrument equipped with a 4.0 mW He-Ne laser operating at a wavelength of 633 nm at room temperature. The energy of molecules and energy gaps are calculated by DFT using Gaussian 09 software was with CAMB3LYP/6-31+G (d,p) as basis

set. For measurements of UV-visible absorptions and fluorescence emissions appropriate 3 ml of each solution in specific solvents in quartz cuvette were measured.

2-(1,4-dioxo-1,4-dihydronaphthalen-2yl-amino)benzoic acid (ANQ) was prepared by reacting 1,4-naphthoquinone with 2-aminobenzoic acid by following procedure: To a well stirred solution of 1,4-naphthoquinone (0.32 g, 2 mmol) in methanol (20 ml) a solution of 2-aminobenzoic acid (0.27 g, 2 mmol) in methanol (10 ml) was drop-wise added. Reaction mixture was stirred overnight and kept at room temperature to slowly evaporate solvent. A dark red precipitate was formed which was filtered and further purified by crystallization from a solution made in N,N'-dimethylacetamide. After five days red crystals were observed Yield : 65%. IR (KBr, cm^{-1}): 3370 (m), 3236 (m), 3060 (w), 2917(w), 1673 (s), 1611 (s), 1584 (s), 1572 (s), 1528 (s), 1453 (m), 1412 (w), 1357 (m), 1296 (s), 1262 (s), 1215 (m), 1151 (m), 1124 (w), 1083 (w), 991 (w), 753 (w), 719 (w). ^{1}H-NMR (600 MHz, CD_3OD): 10.84 (s, 1H), 8.15 (m, 2H), 8.06 (d, J = 6 Hz, 1H), 7.84 (t, J = 12 Hz 1H), 7.77 (t, J = 12 Hz , 1H), 7.69 (m, 2H), 7.23 (m, 1H), 6.65 (s, 1H). ^{13}C NMR (100MHz, DMSO-d_6): 181.9, 178.4, 169.4, 144.3, 139.4, 135.7, 134.9, 133.7, 132.7, 131.8 127.0, 126.5, 126.0, 123.9, 121.2, 117.0, 105.6. Observed HRMS mass (m/e) 294.0792 [M+1]; calculated mass [M+1] for $C_{17}H_{11}NO_4$, 294.0722.

Results and discussion:

The compound ANQ was characterized by recording ^{1}HNMR, ^{13}CNMR, IR, HRMS and determining crystal structure. Compound shows ^{1}HNMR signals of aromatic protons in the region between 7.15 ppm to 8.25 ppm. Assignments of aromatic protons of ANQ recorded in methanol-d_4 are marked in the 2-D HOMO-COSY ^{1}HNMR spectra illustrated in the Fig. 2a. It shows that it remains in methanol as form I as shown in Fig 1. Comparison of ^{1}HNMR spectra recorded in different deuterated solvents showed that chemical shift positions of proton Ha and Ha' and Hb, Hb' (inset of Fig. 2a) are shifted by each solvent to different extents. Signals of H_d and H_f appear as a triplet and a doublet. These signals are less affected by solvents [Figs. 2b(i).-(iv)]. This suggests that solvent influences the resonance structure by affecting intra-molecular hydrogen bond.

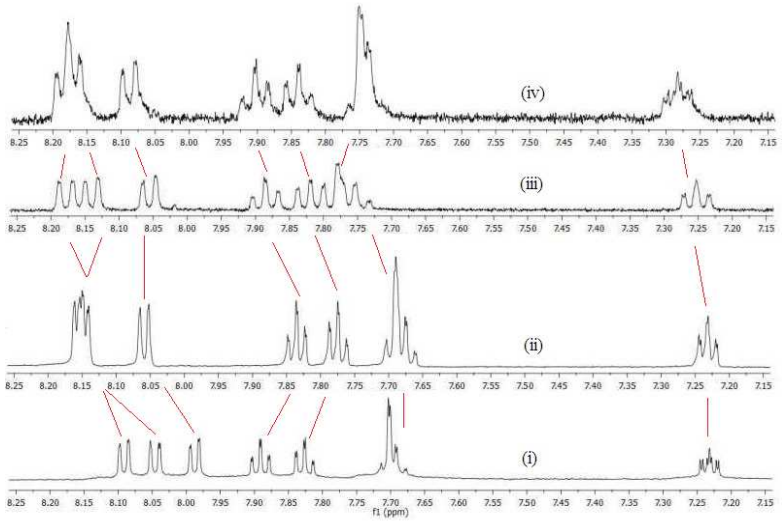

(b)

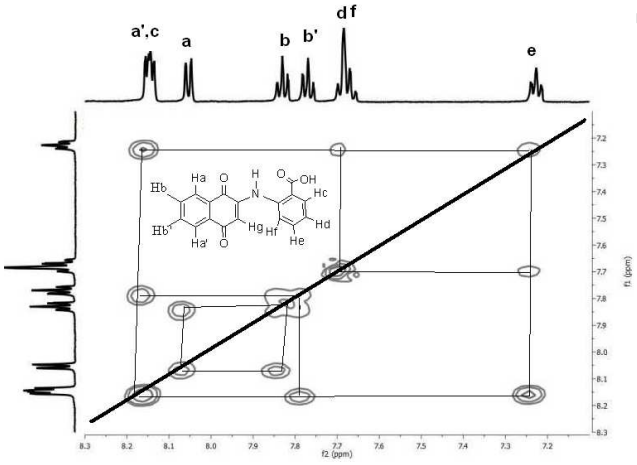

(a)

Fig. 2: (a) 2D-HOMO-COSY ^{1}H-NMR spectra of ANQ in methanol-d_4 in the range 7.00 ppm-8.30 ppm. (b) ^{1}H-NMR spectra (region showing 7.15-8.25 ppm) of ANQ in (i) DMSO-d_6, (ii) Methanol-d_4, (iii) Acetone-d_6 and (iv) Mixture of methanol-d_4 and DMSO-d_6 (2:1 v/v).

Depending on solvent signal for N-H proton appears in the region 10.79-10.87 ppm and carboxylic OH is in offset region hence not observed (supporting Fig. 1S). ^{1}HNMR spectra of the compound in methanol-d_4 has two superimposed doublets for Ha' and Hc. These signals are relatively shielded and split into two distinct doublets in DMSO-d_6. Whereas signal for Ha' was slightly deshielded in acetone-d_6 or in mixture of methanol-d_4 and DMSO-d_6 with respect to peak observed for it in methanol-d_4. On the other hand, signals for Hb and Hb' are deshielded in DMSO-d_6 than corresponding signals in methanol-d_4. The peak for proton Hg appeared as singlet at 6.65 ppm and this signal is insignificantly affected by solvents. Hence, signals of protons attached to naphthoquinone rings are more affected by solvents and splitting patterns of signals of protons on carboxyphenyl unit changes with solvents. The changes in chemical shifts and splitting patterns are attributed to geometrical changes in the

molecule due to stabilization or disruption patters are attributed to the changes caused by solvents of intra-molecular hydrogen bond between the carboxylic acid with the N-H of amine. Accordingly extent of conjugation of N-H group with the naphthoquinone ring as well as the environment of the hydrogen of the carboxyphenyl unit changes with solvents.

Compound ANQ crystallizes as dimethylacetamide solvate. Crystal structure of solvated ANQ shows that it has naphthoquinone backbone tethered to 2-aminocarboxylic acid (Form I of Fig. 1). The C10-O3 and C17-O2 carbon-oxygen double bond distances are 1.23(3) Å and 1.22(3) Å respectively. The C-N bond distances of the compound are 1.41 (4) Å for C7-N1 and 1.37(4) Å for C8-N1 bond. The bond difference between the bond distances of two C-N bonds linking the naphthoquinone and phenyl carboxylic acid indicate that N-H group has delocalization with carboxyphenyl unit. This is also reflected in the cyclic geometry adopted by intra-molecular hydrogen bond between N1-H and O1 as illustrated in figure 3.

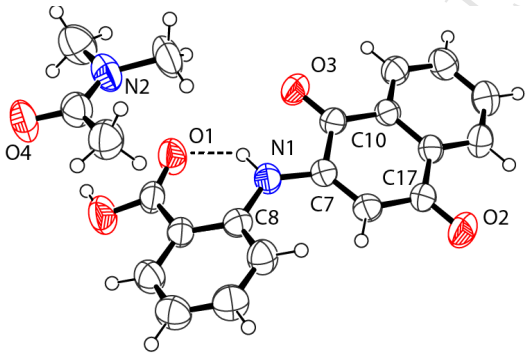

Fig. 3: Structure of dimethylacetamide solvate of ANQ (drawn with 50% thermal ellipsoids)

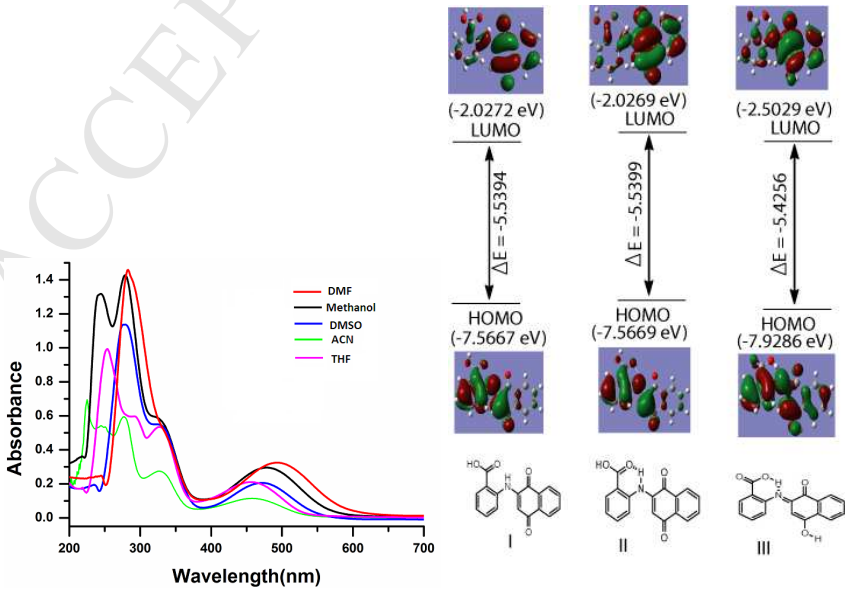

Figure 4: (a) UV-Visible spectra of ANQ (10^{-4} M) in different solvents. (b) HOMO and LUMO and their engegy gaps determined by DFT calculation of diferent forms of ANQ calculated by DFT using CAMB3LYP/6-31+G (d,p) as basis set.

UV-visible spectra of ANQ in methanol shows two equal intensity absorptions at 243 and 279 nm due to π→ π* transitions. Ratio of intensity of these two absorption peaks changes from one solvent to another solvent. This suggests that they originate from contribution from two independent forms (Fig. 4a). In all solvents ANQ consistently showed absorption at 330 nm. In DMSO there were two major absorption peaks at 277 nm and 330 nm due to π→ π* and n→ π* transitions. Wavelength of absorptions along with extinction coefficients of ANQ from spectra recorded in different solvents are listed in Table S1. Each solution showed an absorption in the range of 457 nm to 496 nm. We have also carried out DLS study and found self-aggregation of average particle size 415 nm dimension. Thus, absorption is from the aggregates formed by AQN molecules. Observed peak from charge-transfer in the aggregate is relatively weak in DMSO than methanol. Relative energies of the three forms I-III (Figure 1) are calculated by DFT using CAMB3LYP/6-31+G (d,p) as basis set. It is found that the form I and II has equal energy, whereas naphthoquinone form I has 86.30 KJ/mol lower energy than imino-quinone form III. Energy gaps between HOMO-LUMO of the form I and II are very similar (Fig. 4b). HOMO and LUMO gap of III is smaller than respective energy gaps of other two forms. Quantitatively, the difference in energies of the gaps of I and III is 0.1138 eV (10.98 KJ/mol) whereas difference between such gaps of II and III is 0.1143 eV (11.03 KJ/mol). Symmetry and comparable energy permits interaction of LUMO of III with HOMO of I forming transient charge-transfer species; which provides the basis for CT transition.

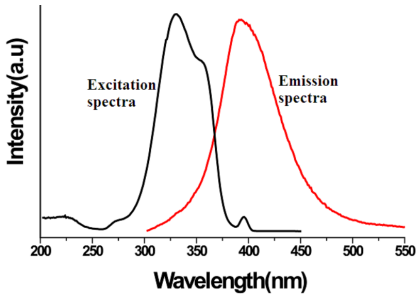

(a)

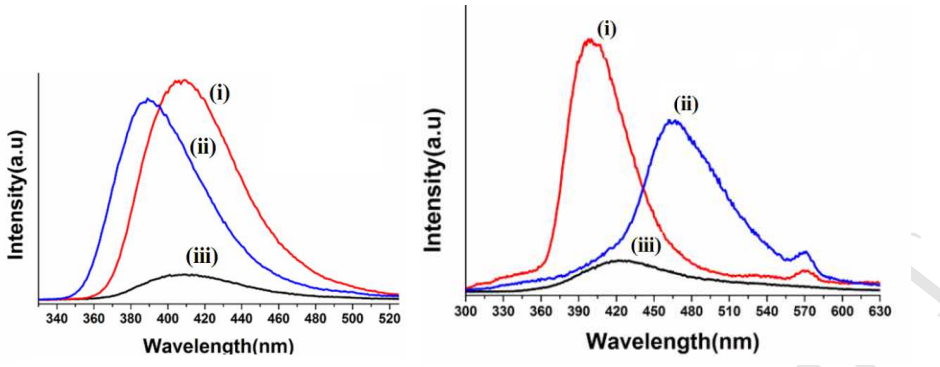

(b) (c)

Fig. 5: (a) Excitation and emission spectra of ANQ in DMF (10^{-4} M, 3 mL) upon excitation at 277 nm. Fluorescence emission of ANQ (10^{-4} M, 3 mL) in (b) MeOH and (c) DMSO at different pH (λ_{ex} in each case 300 nm) in each case (i) pH = 3, (ii) pH = 7, and (iii) pH = 9

Excitation spectra obtained by exciting of a solution of ANQ dissolved in DMF by 277 nm radiation had overlapped excitation peaks due to S_0 to S_1 transitions with vibrational contributions (Fig. 5a). The shapes of such excitation spectra of ANQ recorded in different solvents are distorted in each case. This is due to the vibrational contributions that depend on the solvent polarity and solvation (Supporting Figs. 3S-14S). The probable involvement of excitation from S_0 to S_1+1 state is ruled out as the energy-gap between such states are high (Refer to DFT energy Fig. 22S).

Emission spectra of ANQ obtained upon excitation in UV-region showed single emission at higher wavelength than the corresponding excitation wavelength (Fig. 5a). Fluorescence emission of ANQ in DMF, methanol, DMSO, acetonitrile and THF occur at 389 nm, 405 nm, 403 nm, 390 nm, 388 nm (Fig. 11S) respectively upon excitation at 277 nm. Stoke's shift in each solvent is different, thus emission process occurs through excited state intramolecular proton transfer (ESIPT). Upon change in excitation wavelength within the UV-region, position of emission wavelengths were changed by 1 nm to 2 nm due to involvement of vibrational levels. Though each emission spectrum had single prominent emission, positions of such emissions depend on solvent (Table S1). Relative emission positions were THF < acetonitrile < DMSO < DMF < MeOH which did not follow a trend in solvent polarity THF < DMF < DMSO < acetonitrile < MeOH. These emissions are pH dependent and are quenched in basic condition at pH = 9 (Figs. 5b, 5c). In acidic medium (pH =3) emission in methanol and DMSO solutions has similar Stoke's shifts. For example, excitation at 325 nm

in methanol Stoke's shift is 70 nm, whereas excitation at 330 nm in DMSO it is 78 nm. 1'-Hydroxy-2'-acteophenone is a related system which shows small Stoke's shift and shows ESIPT [51]. It may be noted that in DMSO there is a very weak emission at 570 nm in acidic and in neutral conditions [Fig. 5c(ii)]; this is transition from S_1 to a transient charge transfer state (CT_0), where transient charge transfer interaction between I and III generates CT_0 state. Fluorescence decay of the excitation caused by exciting at 290 nm in methanol has a single decay path with 7.48 ns life-time, whereas similar excitation in DMSO has two life-times 1.84 ns (3.9%) and 8.74 ns (96.1%). The relative intensities of emission peaks also differ at different pH as shown in fig 5b and 5c. In basic medium complete deprotonation of all acidic protons takes place to cause increase in intensity of emission in this region, this is due to extended conjugation. Whereas in neutral condition both the labile protons namely NH and COOH are intact; shows emission from intramolecular hydrogen bonded state. At acidic pH the NH is protonated which disrupts intramolecular hydrogen bond causing quenching of fluorescence.

Excitation at visible region (wavelength > 450 nm) of solutions of ANQ resulted dual emissions in visible region. For example, dual emissions were observed in solvents such as DMF, DMSO, THF, methanol and acetonitrile respectively upon excitation at 504 nm, 500 nm, 471 nm, 488 nm and 471 nm respectively. Differences in intensities of two emission peaks varied from solvent to solvent. Representative excitation and emission spectra of ANQ in DMF upon excitation 500 nm is shown in Figure 6a.

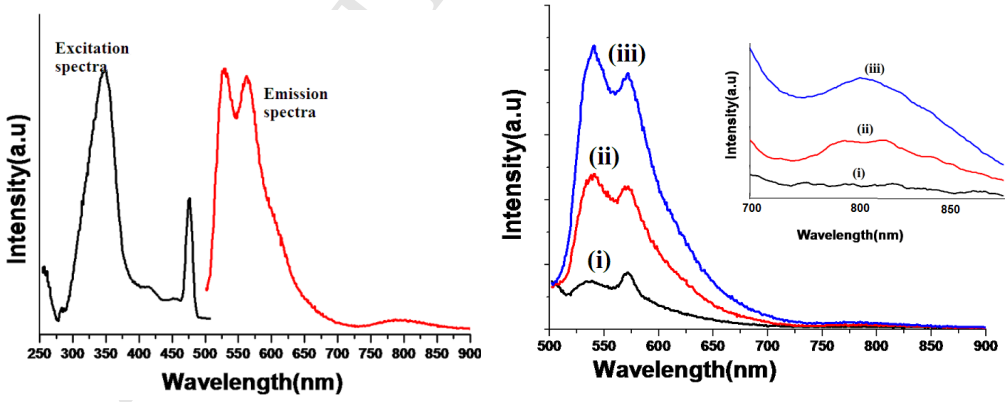

(a) (b)

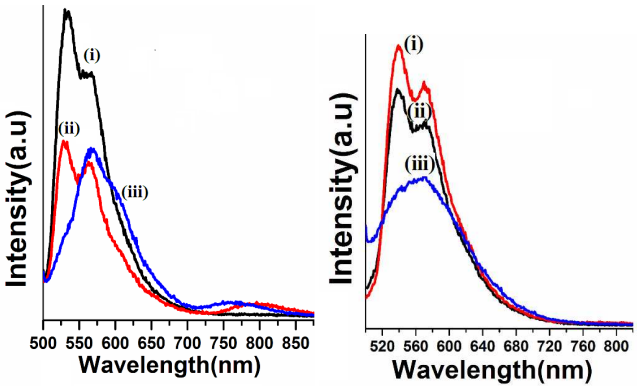

(c) (d)

Fig. 6: (a) Excitation and emission spectra of ANQ in DMF (10^{-4} M, 3 mL) upon excitation at 500 nm. (b) Fluorescence emission of ANQ in DMSO at different concentration (λ_{ex} =500 nm). (i) 10^{-6} M (ii) 10^{-5} M (iii) 10^{-4} M, (3 ml in each case, inset is expansion in 700 to 850 nm)). Fluorescence emission of ANQ (10^{-4} M, 3 mL) in (c) MeOH and (d) DMSO at different pH (λ_{ex} in each case 500 nm) in each case (i) pH = 3, (ii) pH = 7, and (iii) pH = 9.

Excitation spectra were recorded by exciting at wavelengths > 450 in different solvents, they showed similar emission features. They show two emission peaks around 500-600 nm and there is also an emission at 800 nm. The emission peak at 800 nm is highly dependent on concentration and is not observed at lower concentration (Fig. 6b). Based on its occurrence at high wavelength and concentration dependence and absence at low concentration this emission peak is thus attributed to aggregation induced excitation. For example in methanol it had an excitation peak for CT_0-CT_0^* transition at 475 nm (Fig. 6a). There is also excitation peak at 330 nm (Fig. 6a) which is due to excitation of S_0-S_1 of keto or enol form. The emission spectrum under neutral condition in methanol showed two emission peaks at 530 nm and 556 nm. The peak at 530 nm was not observed in basic medium. Thus, the peak at 556 nm is attributed to emission from anion of ANQ. Weak emission around 800 nm was observed in methanol solution under neutral and acidic condition, but this emission was absent in basic condition. This peak is attributed to aggregation induced emission as it is concentration dependent as well as pH dependent. On the other hand, in neutral and acidic pH dual fluorescence were slightly affected but intensities were changed by pH (Fig. 6b, 6c). In basic condition single emission occurs, which is suggests that in basic medium anion are responsible for such emission.

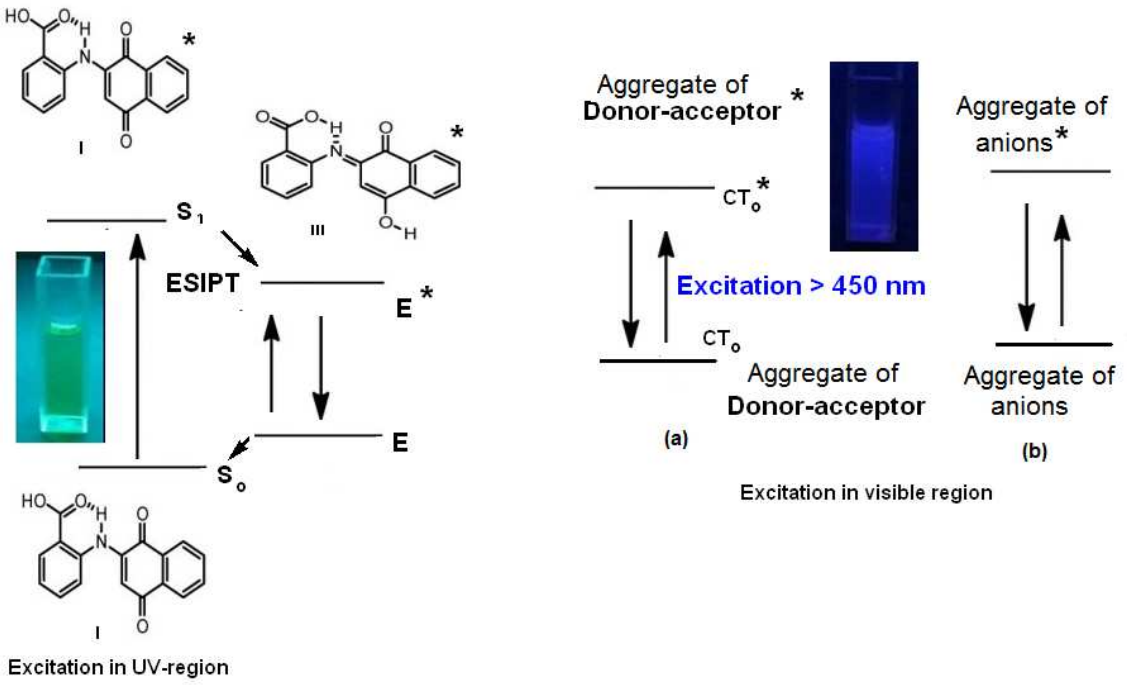

Fig. 7: Mecahnism of single and dual fluoroscence emission shown by ANQ

Life-time of fluorescence decay of ANQ upon excitation at 475 nm in methanol shows two decay paths with life-times 1.69 ns (18.5%) and 4.80 ns (81.5%). On the other hand, a similar excitation in DMSO has two life-times one at 1.52 (25.5%) and other at 4.78 ns (74.5%). This suggests that decay paths in these solvents are similar but different percentages of molecules take independent paths. Entire emission process of ANQ involves contribution of ESIPT and aggregation of ANQ. In case of excitation at short wavelength ESIPT was operative (E* to E of Fig. 7). While upon excitation in longer wavelength caused emission involving charge-transfer as well as anions are involved. In basic medium charge-transfer are reduced hence single emission at visible wavelength is observed. Dual emissions take place by CT_0^*-CT_0 and S_1' to S_0' states of anion. At higher concentration aggregation of ANQ takes place to show aggregation induced emission at 800 nm. Dual fluorescence and excited-state proton transfer in 1,5-dihydroxyanthraquinone was reported earlier. In such example, structured fluorescence pattern at shorter wavelength region, whereas less structured emission at longer wavelengths were observed [52-53]. On the other hand, a recent study has revealed dual emission in dihydroxy-9,10-anthraquinone as consequence of proton transfer [54]. Dual emission in 3-hydroxychromones accompanies proton transfer, where solvents play a major role [55]. Based on these our observations on dual emission involving anion generated under ambient condition facilitated by solvents add value of uncommon dual

fluorescence emission found in ANQ. It also clearly suggests that the substrate dependent single or dual emission [49] of positional isomers by UV-radiations.

This study shows study that concentrations of ANQ in various solvents modulate multiple mode emissions. Single emission caused by ESIPT at higher wavelength than the excitation wavelength and dual emissions due to aggregation leading to charge transfer and anion formation induced emissions are clear from this study. The modulation of multiple modes and understanding their modulation with clear distinctions of emissions upon excitation by visible wavelength source giving detectable color to naked eyes projects such compounds useful for imaging techniques.

Supporting information: Crystallographic information file is deposited to CCDC and it has CCDC No. 1494729. Experimental details, ^{1}H-NMR spectra of ANQ in different solvents, excitation and emission spectra, Fluorescence life-time data of ANQ, theoretical data of DFT are available.

Acknowledgements: The authors thank Ministry of Human Resources and Development, India for financial support (Grant No. F. No. 5-1/2014-TS.VII).

References:

1. T. Ueno, T. Nagano, Nature Methods 8 (2011) 642-644.

2. G. K. Walkup, B. Imperiali, J. Am. Chem. Soc. 119 (1997) 3443-3450.

3. G. Gilardi, L. Q. Zhou, L. Hibbert, A.E. Cass, Anal. Chem. 66 (1994) 3840-3847.

4. M. Machacek, L. Hodgson, C. Welch, H. Elliott, O. Pertz, P. Nalbant, A. Abell, G. L. Johnson, K. M. Hahn, G. Danuser, Nature 461 (2009) 99-103.

5. Z. Omidvar, K. Parivar, H. Sanee, Z. Amiri-Tehranizadeh, A. Baratian, M. R. Saberi, A. Asoodeh, J. Chamani, J. Biomol. Struct. Dynamics, 29 (2011) 181-206.

6. M. M. Moghaddam, M. Pirouzi, M. R. Saberi, J. Chamani, Luminescence 29 (2014) 314-331.

7. R. L. Nicholson, M. Welch, M. Ladlow, D. R. Spring, ACS Chem. Biology 2 (2007) 24-30.

8. A. Shivalingam, M. A. Izquierdo1, A. Le Marois, A. Vysniauskas, K. Suhling, M. K. Kuimova, R. Vilar, Nature Commun. **6** (2015) Article number: 8178

9. S. Rashidpour, S. Naeeminejad, J. Chamani, J. Biomol. Struct. Dynamics, 34 (2016), 57-77.

10. B. R. Jali, Y. Kuang, N. Neamati, J. B. Baruah, Chemico-Biological Interactions 214C, (2014) 10-17.

11. P. R. Rich, Faraday Discuss. Chem. Soc. 74 (1982) 349-364.

12. V. -C. Niculescu, N. Muresan, A. Salageanu, C. Tucureanu, G. Marinescu, L.Chirigu, C. Lepadatu, J. Organomet. Chem. 700 (2012) 13-19.

13. C. Roy, D. Lancaster, H. Michel, Structure 5 (1997) 1339-1359.

14. Function of Quinones in Energy Conserving Systems edited by B. Trumpower, Academic Press, (1982).

15. G. Cecchini, E. Maklashina, V. Yankovskaya, T. M. Iverson, S. Iwata, FEBS Lett. 545, (2003) 31-38.

16. D. Gust, T. A. Moore, A. L. Moore, Acc. Chem. Res. 26 (1993) 198-205.

17. M. R. Wasielewski, Chem. Rev. 92 (1992) 435-461.

18. A. Rybina, B. Thaler, R. Kramer, D. -P. Herten, Phys. Chem. Chem. Phys. 16 (2014) 19550-19555.

19. R. Bergonzi, L. Fabbrizzi, N. Licchelli, C. Mangano, Coord. Chem. Rev. 170 (1998) 31-47.

20. M. Kadarkaraisamy, A.G. Sykes, Inorg. Chem. 45 (2006) 779-786.

21. I. Moczar, P. Huszthy, A. Mezei, M. Kadar, J. Nyitrai, K. Toth, Tetrahedron 66 (2010) 350-358.

22. K. Yoshida, T. Mori, S. Watanabe, H. Kawai, T. Nagamura, J. Chem. Soc., Perkin Trans.*2*, (1999) 393-398.

23. R.M. F. Batista, E. Oliveira, S.P.G. Costa, C. Lodeiro, M.M.M. Raposo, Org. Lett. 9, (2007) 3201-3204.

24. K. Yoosaf, B. I. Ipe, C. H. Suresh, K. G. Thomas, J. Phys. Chem. C 111 (2007) 12839-12847.

25. S. -P. Wu, R.-Y. Huang, K. -J. Du, Dalton Trans. (2009) 4735-4740.

26. J. Q. Chambers, Electrochemistry of quinones, in The Chemistry of Quinonoid Compounds, S. Patai and Z. Rappoport, Eds., vol. 2, chapter 12, pp. 719-757, Wiley, New York (1988).

27. J. Q. Chambers, Electrochemistry of quinones, in The Chemistry of Quinonoid Compounds, S. Patai and Z. Rappoport, Eds., vol. 1, chapter 14, pp. 737-791, Wiley, New York (1974).

28. F. S. Miranda, C. M. Ronconi, M. O. B. Sousa, G. Q. Silveira, M, D. Vargas, J. Braz. Chem. Soc. 25, 2014, 133-142.

29. P. R. Dandawate, A. C. Vyas, S. B. Padhye, M. W. Singh, J. B. Baruah, Mini Rev. Med. Chem. 10 (2010) 436-454.

30. L. Yuan, W. Lin, K. Zheng, L.He, W. Huang, Chem. Soc. Rev., 42 (2013) 622-661.

356 31. C. V. Kumar E. H. Asuncion, J. Am. Chem. Soc. 115 (1993) 8541-8553.
357 32. A. M. Pizarro, A. Habtemariam, P. J. Sadler, Top. Organomet. Chem. 32 (2010) 21-56.
358 33. P. Scharf, J. Muller, ChemPlusChem 78 (2013) 20-34.
359 34. L. Ronconi, P. J. Sadler, Coord. Chem. Rev. 251 (2007) 1633-1648.
360 35. C. V. Kumar, E. H. Asuncion, J. Chem. Soc. Chem. Commun. (1992) 470-472,
361 36. P. Pandya, Md M. Islam, G. Sureshkumar, B. Jayaram, S. Kumar, J. Chem. Sci. 122,
362 (2010) 247-257.
363 37. M. Coll, J. Aymami, G. A. van der Marel van Boom J. H. A. Rich, A. H. J. Wang,
364 Biochem. 28 (1989) 310-320.
365 38. J. L. Dimicoli, C. Helene, Biochem. 13 (1974) 714-723.
366 39.H. Shiozaki, M. Matsuoka, J. Mol. Struct.(Theochem) 427 (1998) 253-261.
367 40. B. R. Jali, J. B. Baruah, ChemPlusChem 78 (2013) 589-597.
368 41. B. R. Jali, J. B. Baruah, Dyes and Pigments 110 (2014) 56-66.
369 42. G. Jones, II and X. Qian, J. Phys. Chem. A 102 (1998) 2555-2560
370 43. S. H. Cho, H. Huh, H. M. Kim, C.I. Kim, N. J. Kim, S. K. Kim, J. Chem. Phys. 122
371 (2005) 034304.
372 44. W. Rettig, Angew. Chem. Int. Ed. Eng. 25 (1986) 971-988.
373 45. W. Rettig, M. Maus, in “Conformational Analysis of Molecules in Excited States”, ed. J.
374 Waluk, Wiley-VCH, New York, Methods in Stereochemical Analysis Series, (2000) p. 1-55.
375 46. W. Rettig in "Modern Models of Bonding and Delocalization", J. Liebman and A.
376 Greenberg, Ed., VCH Publishers, New York, (1988) ch 5, p. 229-282.
377 47. L. P. Fieser, J. Am. Chem. Soc. 50 (1928) 439-465.
378 48. S. Bhand, R. Patil, Y. Shinde, D. N. Lande, S. S. Rao, L. Kathawate, S. P. Gejji, T.
379 Weyhermüller, S. Salunke-Gawali, J. Mol. Struct. 1123 (2016) 245-260.
380 49. M. P. Singh, J. B.Baruah, J. Fluoresc. (2017) DOI 10.1007/s10895-017-2130-2.
381 50. S. Jana, S. Dalapati, N. Guchhait, J. Phys. Chem. A 117 (2013) 4367-4376.
382 51. J. Catalan, J. C. DelValle, J. Am. Chem. Soc. 115 (1993) 4321-4325.
383 52. M. H. VanBenthem, G. D. Gillispie, J. Phys. Chem. 88 (1984) 2954-2960.
384 53. O. F. Mohammed, D. Xiao, V. S. Batista, E. T. J. Nibbering, J. Phys. Chem. A, 118,
385 (2014) 3090-3099.
386 54. A. N. Diaz, J. Photochem. Photobio. A (Chem) 53 (1990) 141-167.
387 55. A. S. Klymchenko, V.G. Pivovarenko, T. Ozturk, A. P. Demchenko, New J. Chem. 27
388 (2003) 1336-1343.

Highlights

- Dual fluorescence modes of 2-aminobenzoic acid tethered 1,4-naphthoquinone is established.
- Emission in UV or visible region independently caused by varying excitation wavelength.
- Fluorescence emissions are modulated by changing pH, concentration and solvent.
- Single emission upon excitation at UV-region is consequence of ESIPT.
- Dual emissions at visible region are due to contribution from charge-transfer and anions.